ELSEVIER

Catalysis Today 78 (2003) 571–579

CATALYSIS TODAY

www.elsevier.com/locate/cattod

$Ta_yNb_{1-y}VO_5$ ($0 < y < 1$) mixed oxides synthesized by sol–gel method: electrochemical Li^+-insertion

J.M. Amarilla*, M.L. Pérez-Revenga, B. Casal, E. Ruiz-Hitzky

Instituto de Ciencia de Materiales de Madrid (CSIC), Cantoblanco, 28049 Madrid, Spain

Abstract

Mixed oxides of general formulae $Ta_yNb_{1-y}O_5$ ($0 < y < 1$) have been synthesized by a modified sol–gel method. Characterization of the samples has been carried out by x-ray diffraction, SEM/EDX, FTIR spectroscopy and thermal analysis. The electrochemical properties have been studied in a lithium cell. The first discharge capacity decrease from 206 ($y = 0.25$) to 136 mA h g^{-1} ($y = 0.75$). $Ta_yNb_{1-y}O_5$ samples undergo an irreversible structural changes induced by electrochemical Li^+-insertion. For all compositions, the new compounds formed after the first discharge has a very high cyclability, as shown the low capacity loss <1% per cycle.

Keywords: Sol–gel; Group V; Nb; Ta; V; Lithium batteries; Cathode oxides

1. Introduction

Oxides in which the metal element have d^0 electronic configuration (i.e. group V metals) can show intrinsic insulating or semi-conducting properties, whereas partial reduction of the lattice and/or inclusion of electron donors into the host lattice can change their electronic properties [1]. Insertion reactions can only be carried out if the host lattice has both a crystallographic and electronic structure able to simultaneously accept ions and electrons, respectively. In this sense, it is largely known the ability of the lamellar vanadium oxide xerogels ($V_2O_5{\cdot}1.5H_2O$) to intercalate ionic and molecular species between the charged structural layers and also promote intra-crystalline catalytic reactions [2–5]. Moreover, the coexistence of two or more metals in the composition of the oxide can provide an advantage, since the associated electronic structure could improve the final properties with respect to the parent oxides.

In previous works [6,7], we have applied successfully the sol–gel methods to the synthesis of a new family of mixed oxides belonging to the Group V elements (V–Nb–Ta–O system), characterized as orthovanadates of Ta and/or Nb. This new family of binary or ternary oxides presents a structure in which single VO_4 tetrahedral share corner with MO_6 octahedral (M = Nb, Ta), building structural empty tunnels along the [0 1 0] direction (Fig. 1). The presence of empty channels in the structure and the existence of transition metal elements with high oxidation state in these oxides are promising factors to the use of these vanadium-based oxides as host structure in insertion reactions.

Single and mixed oxides of vanadium have been studied in view to its applications as positive electrode in commercially developed rechargeable lithium batteries [8,9]. Orthorhombic V_2O_5 is limited by the loss of capacity for reversible insertion and low electronic

* Corresponding author.
E-mail address: amarilla@icmm.csic.es (J.M. Amarilla).

0920-5861/02/$ – see front matter
PII: S0920-5861(02)00356-5

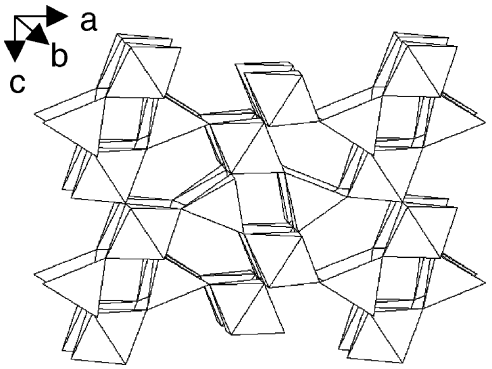

Fig. 1. Structure of $Ta_yNb_{1-y}VO_5$ ($0 < y < 1$) ternary oxides along the [0 1 0] direction.

conductivity. To improve the electrochemical performances of vanadium-based electrodes, on one hand, different non-stoichiometric single oxides as V_6O_{13} as wells as different vanadium mixed oxides have been proposed as positive electrodes [10], on the other hand, several low temperatures methods, as sol–gel [11,12], have also been proposed as alternative to most classical solid-state reaction.

This work is focused towards the study of the electrochemical properties of $Ta_yNb_{1-y}VO_5$ ($0 < y < 1$) prepared via sol–gel in order to test their potential applications as electrodes in lithium batteries. Results about influence of the composition on the capacity and cyclability of ternary oxide are presented.

2. Experimental

2.1. Starting materials

Vanadyl tritertbutoxide, $(^tBuO)_3VO$, was prepared in a similar way as described in [13], by refluxing for 6 h 10 g of orthorhombic V_2O_5 (Aldrich, 99.6%) and 50 ml of tert-butanol (Fluka, >99.7%). The supernatant was recuperated by centrifugation (11 400 rpm, 20 min) and filtering two times trough Schleicher and Schuell, GF92 glasfasser vorfilter 100 stück 0.3 μm. The resulting product ($(^tBuO)_3VO/^tBuOH$), in which the vanadium content was determined by ICP, was used as precursor in the synthesis of the ternary oxides. Niobium pentachloride (Aldrich, 99.9±%) and tantalum pentachloride (Aldrich, 99.99%) were used as received.

2.2. Synthesis of $Ta_yNb_{1-y}VO_5$ ($0 < y < 1$) ternary oxides

Standard experimental procedure was modified from a previous work [6]. Appropriate amounts of the reagents in isopropanol to reach the molar ratio Ta:Nb:V desired, were mixed under magnetic stirring in a dry box to get a homogeneous solution (sol). The resulting sol was poured into Petri dishes in hermetically close container with an initial relative humidity of 100%. After gelation (ca. 4 h), the gel (yellow) was dried in air, obtaining the corresponding precursor xerogel (brown). After powdering it, the xerogel was washed until elimination of Cl^- ions ($AgNO_3$ test) and/or residual organic matter, recovering the solid by centrifugation (11 000 rpm). The product was dried by acetone in air. Finally, the xerogel was crystallized by heating, in air, at 600 °C for 6 h in a platinum crucible.

2.3. Characterization

X-ray powder diffraction (XRD) patterns were recorder with a Phillips PW1010 diffractometer, using Cu Kα radiation. The patterns were scanned at 0.02°(2θ) and 1 s per step counting time within the range $10 \leq 2\theta \leq 80°$. Differential thermal analysis (DTA) and thermogravimetric (TG) curves have been obtained on a Seiko 220U instrument, between 20 and 800 °C in still air, at 10 °C/min heating rate. α-Al_2O_3 was used as reference material. The SEM/EDX studies were carried out using a JEOL JXA 840. The topographical observation was performed by images obtained by secondary electrons. The chemical composition was defined with spectra by dispersion of energy. The EDX microanalyses were carried out using standard specimens of high purity. Both, the observation of the samples and the analyses were performed with 15 KeV voltage of acceleration. The residual pressure was maintained below 10^{-9} Torr. In order to obtain reproducible and representatives results, the images and the analyses were taken in several and different particles, and different point of ones. IR spectra were recorder on a Fourier transform IR (FTIR) Nicolet 20SXC spectrophotometer, on KBr pellets.

The electrochemical properties of $Ta_yNb_{1-y}VO_5$ oxides were evaluated using two-electrode Swagelock cells containing a lithium metal foil anode, a

Whatman BSF-80 glass fibre separator, together with an electrolyte of 1 M solution of $LiPF_6$ in ethylene carbonate and dimethyl carbonate, as supplied by Merck. Composite cathode electrodes were made from the ternary oxide powders (≈15 mg, 70 wt.%), super P carbon black (25 wt.%), and ethylene propylene diene monomer binder (EPDM; 5 wt.%). The three components were mixing by magnetic stirring in cyclohexane, in which the EPDM was dissolved. Then, cyclohexane was evaporated at room temperature, and the solid was cold pressed in circular pellets (13 mm diameter). The Swagelock cells were assembled within an argon glove box in which the water content was kept below 1 ppm. To study the lithium electrochemical insertion/extraction, the cells were submitted at two galvanostatic cycles at C/24 in the voltage range from 1.5 to 4 V. The low current used ensured a quasi-equilibrium response. The rechargeability of $Ta_yNb_{1-y}VO_5$ was determined by galvanostatic cycling at C/5 for discharge and C/8 for charge processes in the voltage range of 1.5–4 V. C is the theoretical capacity of the composite electrode assuming an insertion of one lithium per metallic atom. Galvanostatic studied were run by using an Arbin battery tester (BT-2046).

3. Results and discussion

Sol–gel processes have become a useful method to synthesize new phases of single or mixed oxides via low temperature techniques. The hydrolysis of the reagents used as precursor of the mixed oxides was revealed as a determinant step in the sol–gel processes [11]. In the "sol" state the close mixture of the reagents promotes, through hydrolysis and condensation reactions, the development of a homogeneous inorganic network precursor of the crystalline phases. High dilution conditions as well as a careful control of the relative addition rates of the reagents, in view of their different hydrolysis speed, were also taken as a rule in the synthesis of the $Ta_yNb_{1-y}VO_5$ triple oxides [6]. Therefore, as we referred in a previous work [7], different experimental conditions were tested in order to obtain pure binary oxides in the system Nb–V–O, avoiding the formation of undesired by-products resulting of the homo-polymerization of the reagents. These systematic studies shown that the gelation process takes place even if water is not added as initial reagents, and $NbVO_5$ was always obtained as single phase. Take into account these results, in the present work we have introduced some modifications on the synthesis process of ternary oxides, which simplify the operative mode. In this way we have observed that precursor xerogels, able to give single phases, can also be obtained in absence of initial water by a simultaneous addition of the reagents in high dilution conditions (1:100 molar ratio reagent/^{i}PrOH), In this way, the experimental kit necessary to control the rates of addition of the reagents (pumps) is avoided. In these conditions, the gelation time (ca. 4 h) is significant lower than the values obtained following the standard procedure before described [6]. After drying and washing, the xerogels obtained are amorphous materials (Fig. 2).

Thermal analysis (TG and DTA curves) recorder from the xerogel given us information about the crystallization temperature of the ternary oxide phases. As example, in Fig. 3 the TG and DTA curves corresponding to $Ta_{0.5}Nb_{0.5}VO_5$ xerogel (25–650 °C) is shown. The mass loss up to 500 °C is assigned to

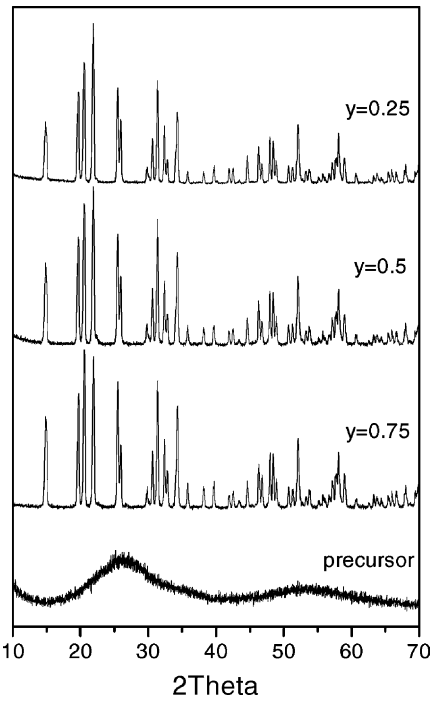

Fig. 2. X-ray diffraction patterns of crystalline $Ta_yNb_{1-y}VO_5$, and $Ta_{0.5}Nb_{0.5}VO_5$ precursor xerogel.

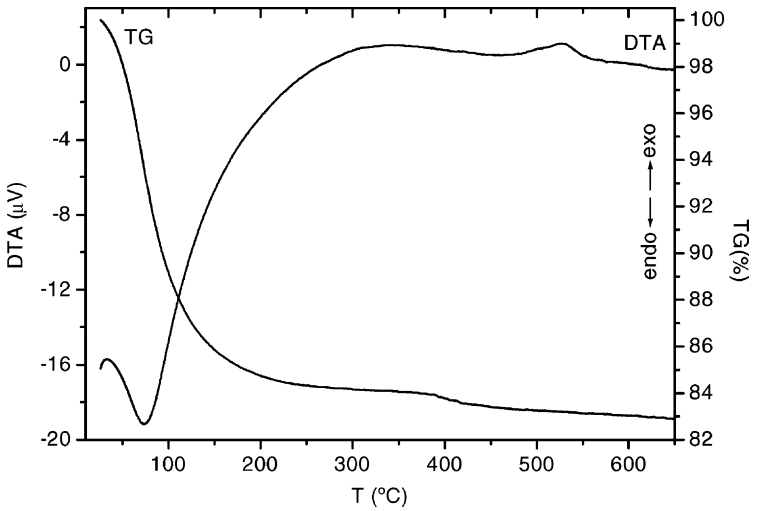

Fig. 3. DTA and TG curves recorded for the $Ta_{0.5}Nb_{0.5}VO_5$ precursor xerogel at 10 °C/min heating/cooling rate in still atmosphere.

the condensation and elimination of water molecules in the process of building up the inorganic network. The strong endothermic effect at 73 °C is due to the removal of water imbibed into the xerogel. The exothermic peak at 528 °C is assigned to the crystallization process of the xerogel, i.e. the formation of the ternary oxide. It is confirmed because this peak is not coincident with either $NbVO_5$, nor $TaVO_5$ binary oxides synthesized also by sol–gel method (424 and 536 °C, respectively) [7]. A similar thermal behaviour is observed for the different composition studied, showing that the crystallization temperature increases as a function of tantalum content (Table 1).

In Fig. 2, the x-ray diffraction patterns of $Ta_yNb_{1-y}VO_5$, obtained after crystallization at 600 °C are plotted. The patterns are the same to those obtained according to the experimental conditions described in [6]. This result corroborates that the ternary oxides have been synthesized as single phases. The similitude of the x-ray patterns reveals that all these compounds are isoestructurals. The differences observed in the intensities of the diffraction peaks are relatives to the different scattering factors of niobium and tantalum. As we discussed elsewhere [6,14] these compounds are also isoestructurals with the MVO_5 (M = Nb, Ta) binary oxides.

Table 1
Thermal analysis (DTA and TG) data of the $Ta_yNb_{1-y}VO_5$ xerogels recorded at 10 °C/min heating rate

Composition	Temperature range (°C)	Mass loss (%)	DTA peaks, T (°C)
$Ta_{0.75}Nb_{0.25}VO_5$	25–400	19.79	Endo: 68
	400–650	2.08	Exo: 530 (sh)[a], 572
$Ta_{0.5}Nb_{0.5}VO_5$	25–650	15.9	Endo: 73 Exo: 528
$Ta_{0.25}Nb_{0.75}VO_5$	2–650	16.8	Endo: 75 Exo: 463, 515

[a] Shoulder.

Fig. 4 shows the SEM/EDX results of $Ta_{0.5}Nb_{0.5}VO_5$. Particles with similar morphology and a heterogeneous size, both of them defined and limited for the manual powder processing, are observed. In the same way, similar images are obtained for the others compositions. On the other hand, and in every case, from the analysis of the EDX spectra is took a homogeneous composition of V, Nb, Ta and O elements, indicative of single phases.

The FTIR spectra were recorder in order to compare the transmission bands as a function of the relative amount of the Ta or Nb in the ternary oxides as well as to determine the possible presence of residual organic mater in the precursor xerogel. In Fig. 5, it is shown the FTIR spectra (4000–500 cm^{-1}) of $Ta_{0.75}Nb_{0.25}VO_5$ after and before the thermal treatment. The broad band observed in the spectrum of the precursor xerogel, with a maximum at about 3400 cm^{-1} together with the band at 1620 cm^{-1}, assigned to the stretching ν (O–H)

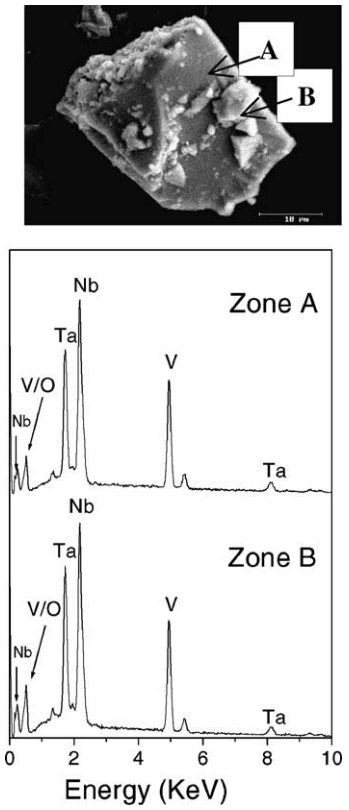

Fig. 4. SEM micrograph and EDX analysis of $Ta_{0.25}Nb_{0.75}VO_5$.

or bending $\delta_{(H–O–H)}$ of the water molecules, respectively, disappear after the crystallization of the oxide. Certainly, thermal analysis (Table 1) corroborates that aspect, because the main loss mass observed in the TG curves takes place in the range 25–200 °C (water loss). On the other hand, absence of bands at about 1400–1200 cm^{-1} is indicative of the negligible amount of organic species in the xerogel, i.e. the alcoholic residues derived from the hydrolysis of the $(^tBuOH)_3VO$ and/or the excess of the ^tBuOH reagent.

Fig. 6 shows the FTIR spectra on the region 1250–250 cm^{-1} of the crystalline mixed oxides as a function of their composition. This region, characteristic of the stretching mode vibrations of M–O groups, is also strongly affected by the structure and morphology of the compounds [15]. As a comparison, we have also represented the FTIR corresponding to the MVO_5 (M = Nb, Ta). As we discussed elsewhere [6], overlapping of the characteristic vibrations of Nb–O and Ta–O groups avoids an accurate assignment of all the bands in these region. Nevertheless, we can observed in all the spectra an intense band centred at about 800 cm^{-1}, which can be attributed to the ν_3 mode of vibration of VO_4 species together with a shoulder at about 920 cm^{-1} attributed to the ν_1 mode of the orthovanadate [16]. This last mode is IR active when a distortion of the XY_4 tetrahedral groups occurs [17]. Bands at about 730 and 670 cm^{-1}, attributed to stretching vibrations of Nb–O or Ta–O

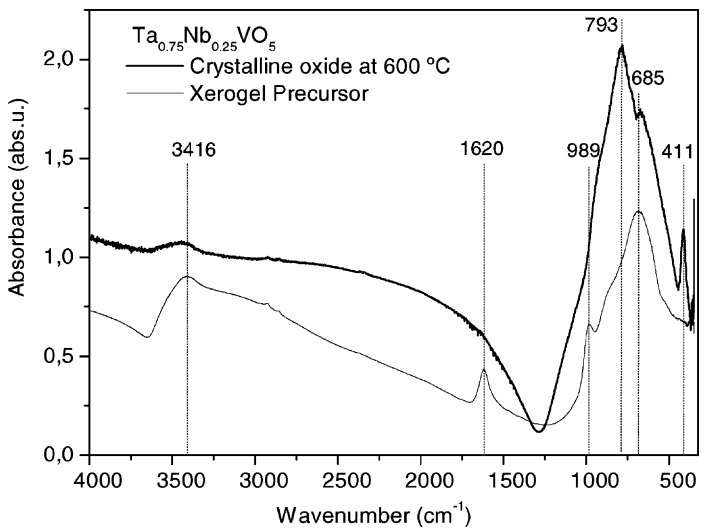

Fig. 5. FTIR spectra of a $Ta_yNb_{1-y}VO_5$ sample after and before thermal treatment.

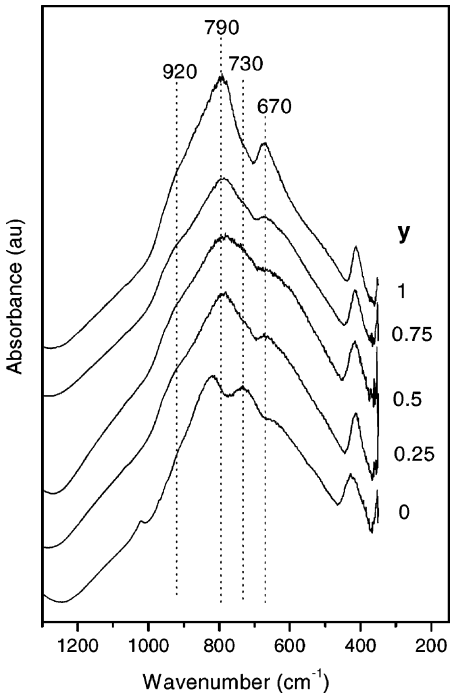

Fig. 6. FTIR spectra of the crystalline $Ta_{0.75}Nb_{0.25}VO_5$ mixed oxides.

groups, respectively, change its relative intensity in function of the composition of the oxide.

Fig. 7a illustrates the charge/discharge curves of the two cycles carried out with Li//$Ta_{0.25}Nb_{0.75}VO_5$ cell, at the very slow current of C/24, in the 1.5–4 V voltage range. The discharge capacity of the first cycle, 206 mA h g^{-1}, corresponds to 1.89 Li^+ inserted. This value, close to one Li^+ per metallic atom, is similar to those reported for other vanadium mixed oxides (see Table 5 in [7]). The discharge capacity of the second cycle ($Q_{disch.}$ = 131 mA h g^{-1}) is notably smaller than that of the first cycle. In addition, the shape of discharge curves is very different. This latter fact is better observed in Fig. 7b in which $-(dq/dV)$ versus voltage is plotted. The differential capacity curve of the first discharge shows several peaks indicating that the lithium insertion into $Ta_{0.25}Nb_{0.75}VO_5$ takes place in different steps. Nevertheless, the derivative curve for the second cycle only shows a very broad peak between 3.5 and 1.8 V. It indicates that the Li^+-insertion takes place only in one step but it is spread in a wide potential range. Differences between first and second discharges are detected in all the others compositions, and for MVO_5 (M = Nb, Ta) binary oxides [7]. All these results allow us to conclude that $Ta_yNb_{1-y}VO_5$ ($0 \leq y \leq 1$) oxides undergo an irreversible structural transformation during the electrochemical lithium insertion to 1.5 V. From x-ray diffraction studies of Li_xNbVO_5 samples, we showed that high values of Li^+-intercalation induce a transition towards amorphous compounds [7]. So, it is reasonable to think that a similar structural evolution would occur in the case of ternary oxides.

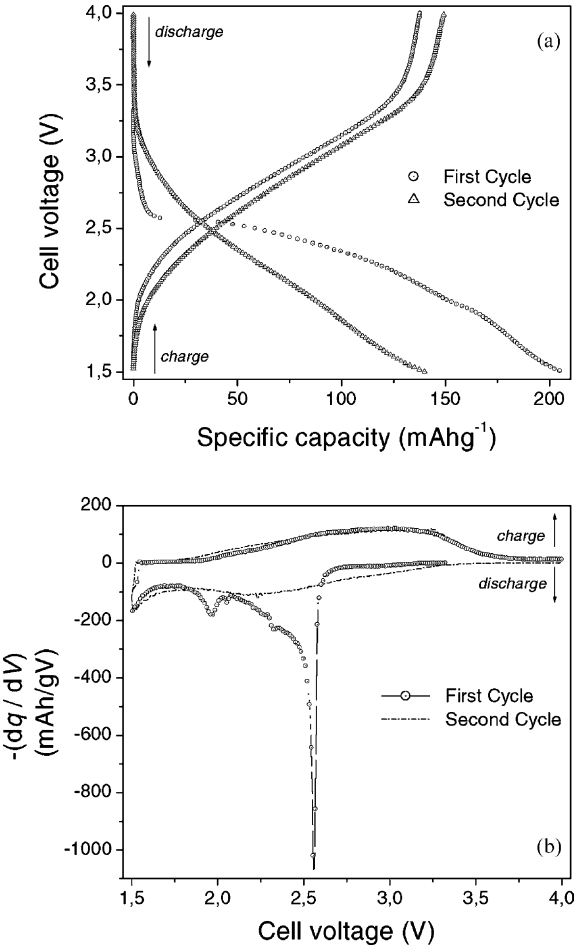

Fig. 7. Charge/discharge curves registered for the first and the second cycle of $Ta_{0.25}Nb_{0.75}VO_5$ at C/24 constant current (a), and corresponding differential capacities curves (b).

In Table 2 the charge/discharge capacities of $Ta_yNb_{1-y}VO_5$ for the two cycles are summarized.

Table 2
Charge (Q_{charge}) and discharge ($Q_{disch.}$) capacities, and insertion degree (x) for $Ta_yNb_{1-y}VO_5$ ternary oxides determined by galvanostatic cycling at C/24 in the voltage region from 1.5 to 4 V

y in $Ta_yNb_{1-y}VO_5$	First $Q_{disch.}$ (mA h g^{-1})	x in $Li_xTa_yNb_{1-y}VO_5$ first discharge	First Q_{charge} (mA h g^{-1})	Second $Q_{disch.}$ (mA h g^{-1})	Second $Q_{charge.}$ (mA h g^{-1})
0[a]	233	1.95	–	–	–
0.25	206	1.89	138	131	138
0.5	158	1.58	103	97	106
0.75	136	1.47	92	85	90
1[a]	135	1.57	–	–	–

[a] Data recorded at C/50 [7].

Data of MVO_5 (M = Nb, Ta) from [7] are included for comparison. For the two cycles, charge/discharge capacities increase as the tantalum content decrease. If it is supposed that the lithium insertion degree (x) is the same for all compositions, the increase on capacity may be explained by a reduction of the molecular weight of the ternary oxides as the tantalum content decreases. The lithium insertion degree reached after the first discharge is indicated in Table 2. If only the V^{5+} is reduced to V^{4+}, the maximum insertion degree would be $x = 1$. In every case, x value is higher than 1. In consequence, in addition of V^{5+}, the Nb^{5+} and/or Ta^{5+} are also reduced during the lithium insertion. In favour of this hypothesis, ESCA studies of $Li_xNb_{1.5}V_{0.5}O_5$ samples showed that V^{5+} and Nb^{5+} ions of the oxide are simultaneously reduced during the lithium electrochemical insertion [18]. As in the case of the specific capacity, the insertion degree increases as the tantalum content decreases (Table 2). This fact can be explained by (i) the lower insertion degree (x) of the tantalum rich samples related to those observed for the niobium analogues and (ii) the atomic mass of the tantalum, double of that of niobium. Both parameters act over the specific capacity, which is directly dependent on the charge content per mass unit.

Opposite to the observed for the discharge steps, the charge capacities of both cycles are very close (Table 2). In addition, the shape of curves is very similar (Fig. 7). indicating that the new Li-intercalation compound, which is formed after the first discharge, is equivalent to that obtained after the second discharge. Moreover, it seems to indicate that the lithium extraction/insertion processes in this new compound have a good reversibility.

The study of the cycling performance of $Ta_yNb_{1-y}VO_5$ oxides has been carried out a moderate constant current, C/5 in discharge. As an example, in Fig. 8 several charge/discharge curves registered during cycling of Li//$Ta_{0.25}Nb_{0.75}VO_5$ cell have been plotted. As for C/24, a noticeable diminution of the discharge capacity from the first to the second cycle is observed. For subsequent cycles, only a slow loss of capacity on cycling is observed. In addition, the shapes of charge/discharge curves are very similar and characterized by a continuous variation of voltage with the lithium content. These kinds of curves are commonly found in amorphous and glass materials [8,19]. X-ray diffraction patterns of composite electrodes after cycling did not show any well-defined peak. This indicates that $Ta_yNb_{1-y}VO_5$ oxides transform to amorphous materials after the first cycle. The slow loss of capacity on cycling indicating that the lithium extraction/insertion from/to these new materials have a very good reversibility. A similar behaviour has been described for the Li^+-insertion in $FeVO_4{\cdot}nH_2O$. The insertion also showed differences between the first and following cycles, which were explained by the amorphization of the structure with the increasing of the lithium insertion degree [8].

In Fig. 9, the variation of the specific capacity versus number of cycles for $Ta_yNb_{1-y}VO_5$ oxides is plotted. As for C/24, the discharge capacity increases with decreasing of the tantalum content. Nevertheless, the capacity at C/5 is ca. 30% lower that C/24 (Table 1). This result indicates that the lithium insertion into $Ta_yNb_{1-y}VO_5$ has noticeable kinetic limitations. In all cases, it is observed a slow loss of capacity on cycling. The loss is larger for the first 20 cycles and subse-

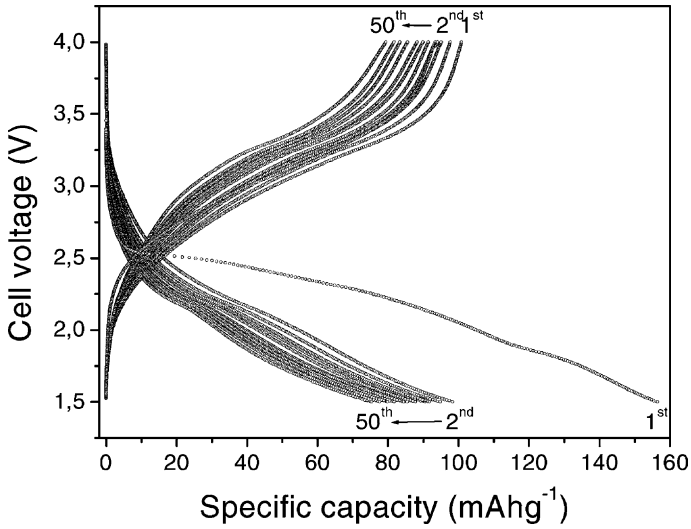

Fig. 8. Charge and discharge curves registered during the cycling of $Ta_{0.25}Nb_{0.75}VO_5$ at constant currents of C/5 for discharge and C/8 for charge.

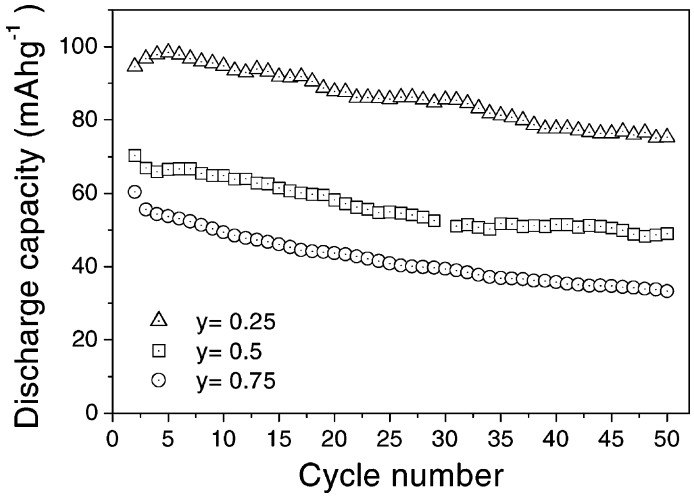

Fig. 9. Evolution of discharge capacity as a function of the number of cycles for $Ta_yNb_{1-y}VO_5$ oxides at C/5 constant current in the voltage region of 1.5–4 V. The discharge capacity of the first cycle has not been included.

quently it decreases. To analyse the cycling behaviour of $Ta_yNb_{1-y}VO_5$ samples, we have assumed a linear decrease of the discharge capacity with the number of cycles. The slopes have been $-0.51\,mA\,h\,g^{-1}$/cycle for $y = 0.25$, and $-0.45\,mA\,h\,g^{-1}$/cycle for $y = 0.5$ and 0.75, respectively. The corresponding loss capacity percentages per cycle have been 0.5, 0.7 and 0.8% for $y = 0.25$, 0.5 and 0.75, respectively. The low values obtained indicate, in every ternary oxide, that the reversibility of the lithium insertion process is very high (>99%). In consequence, $Ta_yNb_{1-y}VO_5$ oxides can act as electrode in rechargeable lithium batteries.

4. Conclusion

Modifications of the sol–gel process previously described for the synthesis of $Ta_yNb_{1-y}VO_5$ have

permitted the preparation of these compounds by a simplified way. The synthesis of the ternary oxides as single phases has been confirmed by x-ray data, thermal analysis and SEM/EDX studies. The Li^+-insertion degree of $Ta_yNb_{1-y}VO_5$ to 1.5 V is close to one Li^+ per metallic atom, and it increases as the tantalum content in the oxide decrease. All ternary oxides undergo an irreversible structural transformation induced by lithium insertion. The new amorphous compounds, formed after the first discharge, exhibit a very high rechargeability as it is shown by the scarce loss capacity percentage (<1% per cycle).

Acknowledgements

Financial support through projects MAT99-1217 and MAT2000-1585-CO3-01 (CICyT) is gratefully acknowledged. M.L.P. thanks to CICyT, project MAT99-1217, for a grant.

References

[1] R. Schöllhorn, Intercalation compounds, in: J.L. Atwood, J.E.D. Davies, D.D. MacNicol (Eds.), Inclusion Compounds, vol. 1, Academic Press, London, 1984.
[2] J. Livage, Chem. Mater. 3 (1991) 578.
[3] M.L. Rojas-Cervantes, B. Casal, P. Aranda, M. Saviron, J. Galván, E. Ruiz-Hitzky, Colloid Poly. Sci. 279 (2001) 990.
[4] B. Casal, E. Ruiz-Hitzky, E. Crespin, M. Tinet, J.C. Galvan, J. Chem. Soc., Faraday Trans. 85 (1989) 4167.
[5] R. Ramírez, B. Casal, L. Utrera, E. Ruiz-Hitzky, J. Phys. Chem. 27 (1990) 8960.
[6] J.M. Amarilla, B. Casal, E. Ruiz-Hitzky, J. Solid State Chem. 99 (1992) 258.
[7] J.M. Amarilla, B. Casal, E. Ruiz-Hitzky, J. Mater. Chem. 6 (1996) 1005.
[8] J.M. Tarascon, Better electrode materials for energy storage applications through chemistry, in: C. Julien, Z. Stonoynov (Eds.), Materials for Lithium-Ion Batteries, NATO Science Series 3, vol. 85, Kluwer Academic Publishers, Dordrecht, 2000.
[9] J.P. Pereira-Ramos, S. Bach, J. Farsi, N. Baffier, Structure and electrochemistry of new lithium intercalation compounds prepared via low temperature techniques, in: C. Julien, Z. Stonoynov (Eds.), Materials for Lithium-Ion Batteries, NATO Science Series 3, vol. 85, Kluwer Academic Publishers, Dordrecht, 2000.
[10] S. Bach, J.P. Pereira-Ramos, N. Baffier, Curr. Top. Electrochem. 4 (1997) 65.
[11] C.J. Brinker, G.W. Scherer, Sol–gel Science: The Physics and Chemistry of Sol–gel Processing, Academic Press, London, 1990.
[12] R.E. Yoldas, J. Mater. Sci. 22 (1977) 1203.
[13] G. Brauer (Ed.), Handbook of Preparative Inorganic Chemistry, 2nd edition, vol. 2, Academic Press, New York, 1965, p. 1271.
[14] J.M. Amarilla, B. Casal, E. Ruiz-Hitzky, J.C. Galvan, Chem. Mater. 4 (1) (1992) 62.
[15] C. Pecharroman, J.E. Iglesias, Appl. Spectrosc. 50 (1996) 1553.
[16] E.J. Baran, M.E. Escobar, Spectrochim. Acta A 41 (1985) 415.
[17] K. Nakamoto, Infrared spectra of Inorganic and Coordination Compounds, Wiley, Chichester, 1963.
[18] N. Kumagai, N. Ikenoya, I. Ishiyama, K. Tanno, Solid State Ionics 28–30 (1998) 862.
[19] J.M. Amarilla, M.T. Colomer, J.R. Jurado, J.L. Acosta, in: Proceedings of the Electroceramic V, Book 2, 1996, p. 223.